Available online at www.sciencedirect.com
ScienceDirect
Biosensors and Bioelectronics 22 (2007) 2065–2070
BIOSENSORS & BIOELECTRONICS
www.elsevier.com/locate/bios

Towards the silicon nanowire-based sensor for intracellular biochemical detection

Inkyu Park [a,b,c,*], Zhiyong Li [c,**], Xuema Li [c], Albert P. Pisano [a,b], R. Stanley Williams [c]

[a] Berkeley Sensor and Actuator Center (BSAC), University of California, Berkeley, CA 94720-1774, United States
[b] Mechanical Engineering Department, University of California, Berkeley, CA 94720-1740, United States
[c] Quantum Science Research, Hewlett-Packard Laboratories, 1501 Page Mill Road, MS 1123, Palo Alto, CA 94304, United States

Received 24 April 2006; received in revised form 5 August 2006; accepted 7 September 2006
Available online 23 October 2006

Abstract

A microneedle sensor platform with integrated silicon nanowire tip was developed for intracellular biochemical detection. Because of the virtue of miniaturized size and high sensitivity, this sensor has a great potential for studying individual cell or localized bioenvironment by revealing the pH level and/or enzyme activities. The fabrication of the microneedle sensor was primarily based on conventional silicon processing, where a silicon-on-insulator (SOI) wafer with 50 nm thick (1 0 0) p-type Si device layer was used as the substrate. The silicon nanowires of 50 nm height and 50–100 nm width were created by electron beam (E-beam) lithography on the tip of microneedle with good electrical connection to the contact pads for convenient electrical measurement. A three layer structure with base, support cantilever, and needle tip was designed to ensure convenient handling of sensors and minimize the invasive penetration into biological cells. In this paper, we demonstrate a preliminary assessment of this novel intracellular sensor with electrical conductance measurement under different pH levels. It is expected that this sensor with proper chemical modification will enable localized biochemical sensing within biological cells, such as neurotransmitter activities during the synaptic communication between neuron cells.

Keywords: Silicon nanowire; In vitro detection; pH sensor; Protein detection

1. Introduction

At present, the study of physiological activities of live organisms in the individual cellular or organelle level is drawing a great attention in various communities such as biomedical science, molecular and cell biology, pharmacology, etc. Representative examples include the monitoring of metabolic processes such as protein synthesis or secretion from individual cells and the detection of neurotransmitters used in communications between nerve cells. Thus far, a number of different approaches have been introduced in the single-cell studies. Fluorescence microscopy has been widely used to detect pH levels (Robey et al., 1998; Olsen et al., 2002), oxygen levels (Ji et al., 2002; Hynes et al., 2003), and ATP contents (Iijima et al., 2003; Kubitscheck et al., 1995) within individual animal cells. However, these optical methods based upon fluorescence can introduce side effects such as interaction between luminescent agents and biochemical molecules in the metabolic processes. Also, the attenuation of optical signals due to photo-bleaching does not allow long-term monitoring of cells.

Alternatives to this optical method are electrochemical sensing by microelectrodes and solid-state device sensing by chemical field effect transistor (ChemFET). Fast-scan cyclic voltammetry (FSCV) with carbon fiber microelectrodes in micron-sized dimensions have been used in the detection of neurotransmitters such as histamine from mast cells (Pihel et al., 1995), dopamine from rat striatum (Bergstrom and Garris, 1999), and catecholamine from chromaffin cells (Wightman et al., 1991). Ion-sensitive field effect transistor (ISFET), a type of ChemFET, has been used to measure the pH level changes by cell metabolism (Baumann et al., 1999; Lehmann et al., 2001).

In this paper, we propose a novel in vitro single cell sensor, which is a microneedle sensor with integrated silicon nanowire sensing components for biochemical detection in intracellular

* Corresponding author. Tel.: +1 510 642 8713.
** Corresponding author.
E-mail addresses: inkyu@eecs.berkeley.edu, inkyupark.ucb@gmail.com (I. Park), zhiyong.li@hp.com (Z. Li).

0956-5663/$ – see front matter © 2006 Elsevier B.V. All rights reserved.
doi:10.1016/j.bios.2006.09.017

or extracellular environments. A few potential advantages of silicon nanowire-based sensor are small quantity of analytes required for sensing, little interference with biochemical processes within cells, compatibility with integrated circuitry, and possibility of multiplexed sensing by distinct surface functionalization on separate nanowire sensors. For the last few years, a number of silicon nanowire sensors have been developed for the chemical detection of pH level, streptavidin (Cui et al., 2001), ammonia or oxygen gas (Zhou et al., 2003; Elibol et al., 2003), DNA (Li et al., 2004, 2005), and proteins such as prostate specific antigen (PSA) (Zheng et al., 2005). The sensing mechanism of silicon nanowire is generally believed to be the change of its electrical conductance upon surface protonation/deprotonation or exposure to charged biological molecules around it. Due to its large surface-to-volume ratio and quasi-1D characteristics, silicon nanowire sensor provides high sensitivity in the analyte detection. As opposed to 2D sensors such as ion sensitive thin film transistor (ISFET) or light addressable potentiometric sensor (LAPS) where the surface charge drives depletion or accumulation of charge carriers only on the surface of the devices, nanowire sensors experiences depletion or accumulation in bulk level. Therefore, sensitivity of sensors can be dramatically improved. Also, by modifying the surface of silicon nanowire, one can functionalize the sensor for detection of various target molecules. However, thus far, most of the silicon nanowire sensor has been developed for the detection of preconcentrated and purified target molecules in buffer solution, while there has been little study about silicon nanowire sensor for in vitro or in vivo detection. In our study, we are pursuing to develop a silicon nanowire-based sensor that can achieve in vitro detection of protein molecules in real-life biological systems. This paper presents our current efforts to this goal in terms of device design, fabrication, and preliminary results of pH level detection by this silicon nanowire sensor based on the surface charge effect.

2. Design and experimental

2.1. Design and theoretical basis

For the intracellular or extracellular biochemical sensing, sharp geometry of sensing electrode is highly desired in order to (1) avoid interference with other individual cells; (2) achieve localized biochemical detection from particular position within/outside of the cells; (3) cause minimal invasiveness to the cell membrane during intracellular detection task. A two step process is designed in this work to make the sharp geometry of microneedle: (1) blunt needle structure definition by photolithography and (2) further sharpening by focused-ion-beam (FIB) machining. Fig. 1(a) depicts the designed structure of the microneedle. On top of this microneedle structure, serpentine pattern of silicon nanowire is defined in order to increase detection length in a small confined area and thus improve the sensitivity of the device. The cross-sectional view of the p-type doped silicon nanowire sensor is shown in Fig. 1(b). As described below, the silicon nanowire in this paper is fabricated by electron beam lithography followed by reactive ion

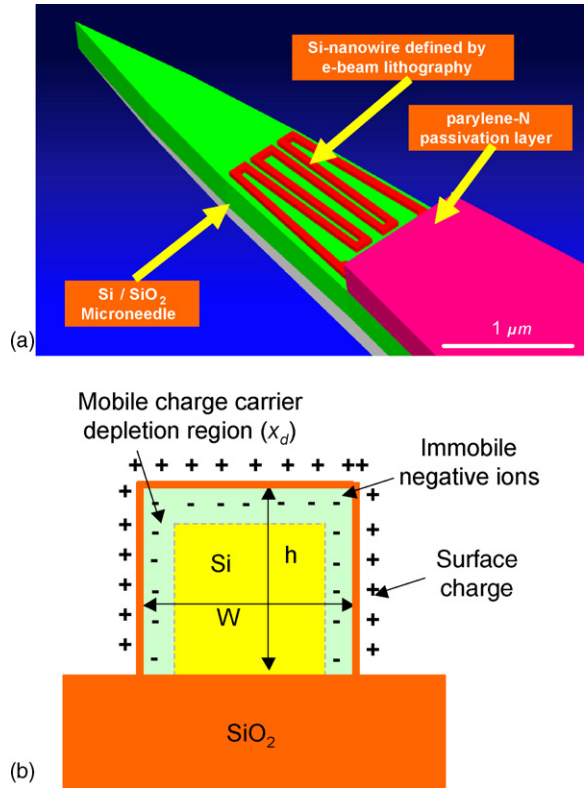

Fig. 1. (a) Design of microneedle tip with integrated serpentine silicon nanowire structure on top surface (b) Cross-sectional view of silicon nanowire fabricated by e-beam lithography on silicon-on-insulator (SOI) substrate.

etching process. Therefore, its cross-sectional geometry will be ideally rectangular. By having a positive surface charge, the mobile charge carriers (holes) become depleted in the perimeter of the silicon nanowire, by which the electrical conductance of the nanowire becomes reduced. For theoretical derivation of the relation between surface charge concentration and electrical conductance, let us assume that the silicon nanowire is doped with p-type dopant (ex. boron) and its concentration is constant. Let W and h be the width and height of nanowire, and N_A be the concentration of doping impurity within the nanowire. If the surface of nanowire is covered with charged molecules with N_S as a net surface charge concentration, the depletion of mobile charge occurs by following equation due to charge neutrality effect:

$$(W + 2h)LN_S = \{2h\Delta x + (W - 2\Delta x)\Delta x\}LN_A \approx (2h + W)\Delta x L N_A$$

where Δx is the thickness of depleted region. The simplification is done under the assumption that the depleted region is much smaller than the width and height of silicon nanowire. By this depletion effect, the effective conduction area is reduced from $A_{\text{conduction,original}} = Wh$ to $A_{\text{conduction,original}} = (W - 2\Delta x)(h - \Delta x) \approx Wh - (W + 2h)\Delta x$

Then, the changed conductance of silicon nanowire can be described as

$$S_{\text{nanowire,depleted}} = \frac{\sigma A_C}{L} \approx \frac{\sigma\{Wh - (W + 2h)\Delta x\}}{L}$$

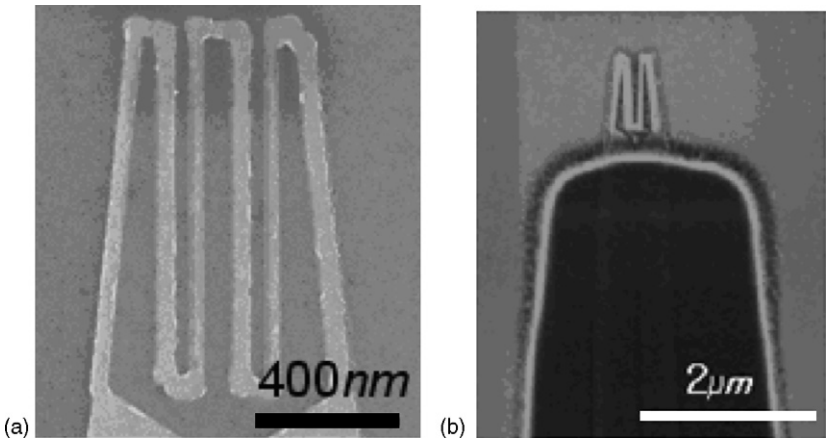

Fig. 2. (a) SEM image of a fabricated silicon nanowire of 50 nm wide on a microneedle and (b) SEM image of a 100 nm wide silicon nanowire with electrochemical passivation by parylene-N thin film (dark region).

Therefore, the relative change of electrical conductance of p-type doped silicon nanowire can be derived as

$$\frac{\Delta S}{S} = -\frac{(W+2h)x_{\mathrm{d}}}{Wh} \approx -\frac{(W+2h)}{Wh}\frac{N_{\mathrm{S}}}{N_{\mathrm{A}}}$$

This equation implies that the electrical conductance decreases as the concentration of surface charge increases, and the sensitivity increases with smaller dimension and lower doping density of silicon nanowire. If there exist negative surface charges, opposite effect is expected. After the fabrication of silicon nanowire by e-beam lithography and reactive ion etching process, its periphery is already depleted by a few nm. Therefore, negative surface charge will reduce the depletion area of mobile charge carrier and increase the electrical conductance as a consequence. Similar theoretical approaches can be found in the literature (Seo et al., 2006). However, the accuracy of this theoretical calculation may be limited if (1) the dopant concentration within the silicon nanowire is not constant due to the dopant redistribution effect; (2) the concentration of surface charge is not constant along the surface of nanowire; (3) the thickness of depleted region is comparable to the dimensions of nanowire.

2.2. Materials and fabrication

Silicon on insulator (SOI) wafer (Soitec, France) with a silicon (Si) device layer thickness of 1000 Å and buried oxide layer of 3800 Å has been used as the substrate of the device fabrication. SiO_2 layer (1100 Å) was thermally grown on the Si device layer to reduce the silicon device layer down to 500 Å. Then, Si device layer was doped with boron by ion implantation (35 keV, 7° tilt, dose = 1.20×10^{14} cm^{-2}) and annealed by rapid thermal annealing at 1025 °C for 60 s. Afterwards, the backside of the wafer was etched by deep reactive ion etching (DRIE). Then, the silicon nanowire pattern was defined by electron beam lithography system and transferred to underlying Si device layer by Cr lift-off and reactive ion etching processes ($CHF_3 + O_2$ for SiO_2 etching and HBr for Si etching). To decrease the density of surface dangling bonds on Si surface and increase the stability of the sensors, a high quality 3 nm SiO_2 layer was grown on Si nanowire surfaces at 925 °C for 1 min in O_2 environment. After selectively etching contact area between Si nanowire and metal interconnect with buffered oxide etchant (HF:NH_4F = 1:10), Al interconnect pattern was defined by photolithography and lift-off process. For the electrochemical passivation of device in liquid environment, the sample was coated with 300 nm parylene-N thin film by vapor phase deposition. This vapor phase deposition process is done by three steps: vaporization of solid parylene dimer (di-*para*-xylylene), pyrolysis of parylene dimer into monomer (*para*-xylylene, and polymerization from monomer to polymer (poly-*para*-xylylene) onto the substrate at room temperature. Afterwards, the tip of microneedle (sensing area) and the area of contact pads were opened by low power O_2 plasma etching (50 W, 300 mTorr, and 50 sccm) of parylene-N thin films with photoresist pattern as an etching mask. Finally the SiO_2 microneedle structure was released by the reactive ion etching of SiO_2 and XeF_2 etching of Si underlying the microneedle structure. The fabrication result of 50 nm silicon nanowire and 100 nm silicon nanowire with parylene passivation are shown in Fig. 2.

2.3. Measurement

After the fabrication of silicon nanowire sensors, we have studied their electrical characteristics by *I–V* measurement with probe station connected to HP4145B semiconductor parameter analyzer. Also, the electrochemical passivation by parylene-N thin film has been analyzed by a computer-controlled electrochemical station (CHI 660A system, CH Instruments, Inc, Austin, TX). Three electrode configuration (Ag/AgCl reference electrode, Pt mesh counter electrode, Au working electrode) with $K_3Fe(CN)_6$ (1 mM) in DI water solution was employed. The impedance spectroscopy was done at sinusoidal excitation voltage of 5 mV between $f = 0.1$ to 10^4 Hz, and cyclic voltammetry was measured under triangular voltage excitation from $V = -1$ to 1 V at a scan rate of 1 V/s. Finally, a preliminary test of silicon nanowire sensor with pH level detection was run by an experimental setup that can provide

a continuous fluidic transport with various buffer solutions in pH levels from pH 2 to 12. These buffer solutions were made by a proportioned combination of phosphoric acid (H_3PO_4), sodium phosphate tribasic dodecahydrate ($Na_3PO_4{\cdot}12H_2O$), sodium phosphate dibasic anhydrous (Na_2HPO_4), and sodium phosphate monobasic monohydrate ($NaH_2PO_4{\cdot}H_2O$). These buffer solutions were carefully prepared using analytical quality chemicals to avoid any potential interference from redox active impurities. The continuous fluidic transport was done by automatic syringe pump through silicon nanowire sensor contained in microchannel machined of polymer polytetrafluoro-ethylene (Teflon®). The electric current was continuously measured across the silicon nanowire sensor with a bias potential of 100 mV, where there is barely any redox reaction that can interfere with pH sensing signal.

3. Results and discussion

3.1. Electrical characterization

We characterized the electrical characteristics of silicon nanowires by *I–V* curve measurement. In general, *I–V* characteristics of silicon nanowire show the behavior of simple linear ohmic resistors with a conductance level in the range of a few tens to a few hundreds of nS. In our process, thermal annealing was performed in forming gas environment (H_2:N_2 = 1:9) at 450 °C after the fabrication of silicon nanowire pattern and contact between Al interconnect and silicon nanowire. The measurement results of *I–V* curves show that the effect of annealing is not only the improvement of ohmic contact between Al and Si, but also the enhancement of electrical conductance through the silicon nanowire. Aside from the silicon nanowire sensor, we made a separate device for the measurement of Al–Si contact resistance. With this device, we have found that total Al–Si contact resistance was reduced from 7.2 to 2.8 kΩ by thermal annealing. However, these contact resistances are much smaller than the total resistance of silicon nanowire sensor (a few hundreds kΩ to a few MΩ depending upon nanowire size) by orders of magnitude. Therefore, it can be concluded that the change of electrical conductance stems mainly from the improvement of electrical conduction across the silicon nanowire, not the region of Al–Si contact. Fig. 3 summarizes the dependence of electrical conductance on the width of nanowire and the thermal annealing. The average electrical conductances for 81 nm nanowire are 7.15 nS and 431 nS before and after thermal annealing, respectively. The average electrical conductances for 129 nm nanowire are 48.4 nS and 1217 nS before and after thermal annealing, respectively. This dramatic change of electrical conductance can be attributed to the process we have chosen to fabricate the silicon nanowire for our device. As mentioned in Section 2.2, the pattern of nanowire was made by e-beam lithography and it was transferred to Si device layer by reactive ion etching (RIE) process. Then, a thin thermal oxide layer was grown in low temperature oxygen environment. The reactive ion etching of SiO_2 by $CHF_3 + O_2$ plasma and Si by HBr plasma can bring surface modification of silicon into complex bonding such as Si–F or Si–O with a thickness of 5–8 nm (Pang et al., 1983; Wilkinson et al., 2002). Also, nonvolatile products of Si and etchant reaction will remain on the surface of silicon nanowire. In addition, during the thermal oxidation process of silicon nanowire, various trapped charges such as oxide trapped charge (Q_{ot}) and interface trapped charges (Q_{it}) can be developed, such that the electrical conduction through the silicon nanowire is inhibited (Plummer et al., 2000). From our measurements, we have found that thermal annealing at 450 °C in forming gas environment attenuates these surface damages and improves the electrical conduction of silicon nanowire by dissipation and neutralization of these surface damages. The electrical conductance is increased by approximately 60 times for 81 nm wide nanowires and 25 times for 129 nm wide nanowires.

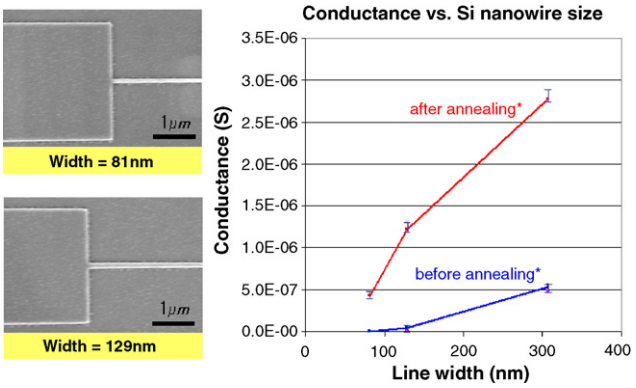

Fig. 3. Electrical conductance of silicon nanowires dependent on the geometrical dimension and thermal annealing condition.

3.2. Electrochemical passivation by parylene-N

Since the biochemical sensing of device is done in aqueous environment such as physiological buffer solution, electrochemical passivation between the electrical conduction path and surrounding environment should be ensured in order to minimize the leakage current and electrical noise, and to avoid redox reaction at the metal surface. In our device, we have chosen parylene-N thin film as the layer for electrochemical passivation since it cannot only provide excellent electrical insulation properties and biocompatibility, but also be deposited very conformally around any micro-topology (Hwang et al., 2004; Fung and Li, 2004; Qu et al., 2004). It also has quite good adhesion and stability on silicon-based surface without the need of intermediate adhesion promoter. However, the thickness of the film is a critical parameter. For intracellular detection, the microneedle should be penetrated through the cell membrane and thus the geometry of the microneedle should be maintained to be sharp. Therefore, it is preferred to keep the passivation layer as thin as possible. On the other hand, thicker passivation layer is desired to have stronger and more reliable electrochemical passivation. In order to resolve this trade-off problem, we have coated parylene-N thin film in different thicknesses (0–1 μm) and compared their electrochemical passivation performances. Fig. 4 shows the results of impedance spectroscopy and cyclic voltammetry. In Fig. 4(a), a 100 nm parylene-N thin film does not enhance the electrochemical impedance, its impedance being

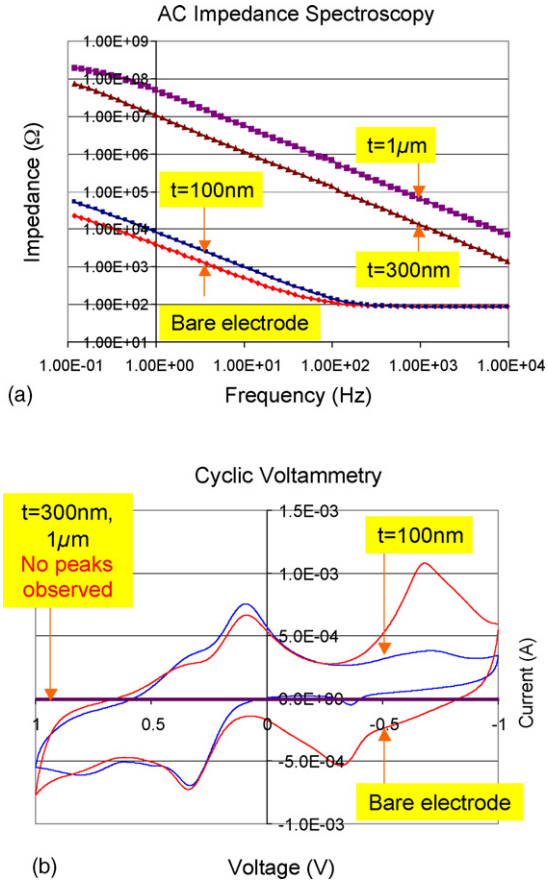

Fig. 4. (a) Impedance spectroscopy and (b) cyclic voltammetry results of parylene-N thin films in different thicknesses with gold working electrode (circular shape with 8 mm in diameter) and 1 mM $K_3Fe(CN)_6$ solution.

only two to three times higher than that of bare gold electrode. However, the impedance of 300 nm thick parylene-N becomes dramatically improved by three orders of magnitude. When the thickness is further increased to 1 μm, the impedance increases only by four to five times. From these results, it is inferred that the drastic jump of electrochemical impedance from 100 to 300 nm thickness originates from the existence of possible pinholes or incomplete coverage of parylene-N thin film in the case of 100 nm thickness whereas this imperfection does not exist in 300 nm film. Slow increase of impedance from 300 nm to 1 μm is attributed simply to the thickening of dielectric material, which increases resistance and decreases capacitance terms in the electrochemical impedance. The saturation of impedance signals over 100 Hz frequency for bare electrode and 100 nm thick parylene from the data is believed to be the limitations of the measurement setup. When the passivation is poor or does not exist, the impedance relies mostly on the electric double layer. If the impedance becomes smaller than the intrinsic impedance of measurement setup, the measured signal is saturated. The great improvement of electrochemical passivation by parylene layer is also confirmed by cyclic voltammetry measurement in Fig. 4(b). In the cases of zero or 100 nm thickness, the reduction/oxidation peaks of $K_3Fe(CN)_6$ electrolyte on Au electrode with an area of 0.7 cm^2 is measured as ~700 μA. On the contrary, in the cases of 300 nm or 1 μm

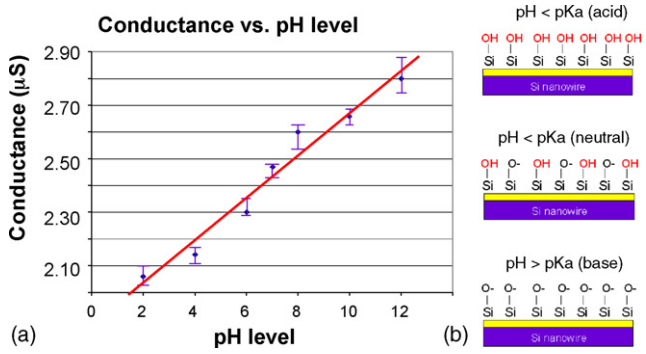

Fig. 5. pH level detection of solution by silicon nanowire sensor. (a) Change of electrical conductance by different solution pH level. (b) Proposed mechanism of electrical conductance change of silicon nanowire under different pH level.

thicknesses, the redox of ferrocyanide is completely blocked by the films, with electrochemical current being in the level of noise. From these results, we have chosen 300 nm as the satisfactory thickness of parylene-N passivation layer for our device.

3.3. pH level detection

In order to prove the usefulness of our silicon nanowire device as a chemical sensor based upon surface charge field effect, we have done preliminary test of the device by pH level detection of the solution. Fig. 5 shows the detection result of pH level by the serpentine silicon nanowire sensor with 100 nm width and 6 μm length. The graph and error statistics were taken from measurement of five individual silicon nanowire sensors. At pH < pK_a, where the concentration of available proton ion (H^+) is high, the electrical conductance is low. On the other hand, when the pH > pK_a, the electrical conductance becomes higher. This shows that the silicon nanowire works well as a chemical sensor based upon the concentration of surface charge around the silicon nanowire. By having more protonation on surface hydroxyl groups and positive surface charges as a result in the range of pH < pK_a, the boron doped p-type Si experiences depletion of mobile charge carriers (holes) around the perimeter of the silicon nanowire. Qualitatively, the less pH value is, the more protonation on the surface, therefore the less conductance in the nanowire. If the solution pH level is above pK_a, the surface hydroxyl groups start the deprotonation process, generating negative ions on the nanowire surface, by which the degree of mobile charge carrier depletion is lessened and furthermore can accumulate more carriers in the nanowire. Consequently, the electrical conductance of silicon nanowire is increased. The sensor roughly shows a linear relationship between pH level and electrical conductance of the nanowire with an approximate sensitivity of 79.4 nS/pH.

From these experimental results, we have verified that this silicon nanowire sensor works well as a chemical field effect sensor and we believe such platform can be generalized for the detection of charged protein molecules with the proper surface functionalization, which is currently under investigation.

4. Conclusion

In this paper, we have discussed our recent development of silicon microneedle with integrated silicon nanowire sensor for the potential application in the detection of biochemicals within or outside of the individual live cells. We have successfully designed and fabricated the device on SOI substrate. The device performance was tested with pH solutions ranging from 2 to 12, and a sensitive pH response with 79.4 nS/pH was achieved in the sensors fabricated.

Acknowledgements

This project has been funded partially by Grant (No. 019997) from Center for Nanoscale Mechatronics and Manufacturing (CNMM), one of the 21st Century Frontier Research Programs, which are supported by Ministry of Science and Technology, Korea. It has also been partially funded by Defense Advanced Research Projects Agency (DAPRA) and HP. The authors also want to thank Dr. Ted I. Kamins and Dr. Wei Wu (HP labs, Palo Alto), Dr. Jie Li and Mr. Byungkook Lim (Molecular and Cell Biology Department, UC Berkeley), and Dr. Jun-Ho Joung and Dr. Eung-Sug Lee (KIMM, Korea) for their discussion, advice, and comments.

References

Baumann, W.H., Lehmann, M., Schwinde, A., Ehret, R., Brischwein, M., Wolf, B., 1999. Sens. Actuators B 55, 77–89.

Bergstrom, B.P., Garris, P.A., 1999. J. Neurosci. Meth. 87, 201–208.

Cui, Y., Wei, Q., Park, H., Lieber, C.M., 2001. Science 293, 1289–1292.

Elibol, O.H., Morisette, D., Akin, D., Denton, J.P., Bashir, R., 2003. Appl. Phys. Lett. 83, 4613–4615.

Fung, C.K.M., Li, W.J., 2004. Proceedings of the 2004th IEEE Conference on Nanotechnology, pp. 158–160.

Hwang, K.S., Park, J.H., Lee, J.H., Yoon, D.S., Kim, S., Han, I., Noh, H., 2004. J. Korean Phys. Soc. 44, 1168–1172.

Hynes, J., Floyd, S., Soini, A.E., O'Connor, R., Papkovsky, D.B., 2003. J. Biomol. Screen. 8, 264–272.

Iijima, T., Mishima, T., Tohyama, M., Akagawa, K., Iwao, Y., 2003. Neurochem. Int. 43, 263–269.

Ji, J., Rosenzweig, J.N., Jones, I., Rosenzweig, Z., 2002. J. Biomed. Opt. 7, 404–409.

Kubitscheck, U., Pratsch, L., Passow, H., Peters, R., 1995. Biophys. J. 69, 30–41.

Lehmann, M., Baumann, W., Brischwein, M., Gahle, H.-J., Freund, I., Ehret, R., Drechsler, S., Palzer, H., Kleintges, M., Sieben, U., Wolf, B., 2001. Biosens. Bioelectron. 16, 195–203.

Li, Z., Chen, Y., Li, X., Kamins, T.I., Nauka, K., Williams, R.S., 2004. Nano Lett. 4, 245–247.

Li, Z., Rajendran, B., Kamins, T.I., Li, X., Chen, Y., Williams, R.S., 2005. Appl. Phys. A: Mater. Sci. Process. 80, 1257–1263.

Olsen, K.N., Buddle, B.B., Siegumfeldt, H., Rechinger, K.B., Jakobson, M., Ingmer, H., 2002. Appl. Environ. Microbiol. 68, 4145–4147.

Pang, S.W., Rathman, D.D., Silversmith, D.J., Mountain, R.W., DeGraff, P.D., 1983. J. Appl. Phys. 54, 3272–3277.

Pihel, K., Hsieh, J.W., Jorgenson, J.W., Wightman, R.M., 1995. Anal. Chem. 67, 4514–4521.

Plummer, J.D., Deal, M.D., Griffin, P.B., 2000. Silicon VLSI Technology: Fundamentals Practice and Modeling. Prentice Hall.

Qu, S.C., Fung, C.K.M., Chan, R.H.M., Li, W.J., 2004. Proceedings of the Fifth World Congress on Intelligent Control and Automation, IEEE Part 6, pp. 5613–5618.

Robey, R.B., Ruiz, O., Santos, A.V., Ma, J., Kear, F., Wang, L.J., Li, C.J., Bernardo, A.A., Arruda, J.A., 1998. Biochemistry 37, 9894–9901.

Seo, K.-I., Sharma, S., Yasseri, A.A., Stewart, D.R., Kamins, T.I., 2006. Electrochem. Solid-State Lett. 9, G69–G72.

Wightman, R.M., Jankowski, J.A., Kennedy, R.T., Kawagoe, K.T., Schroeder, T.J., Leszczyszyn, D.J., Near, J.A., Diliberto Jr., E.J., Viveros, O.H., 1991. Proc. Natl. Acad. Sci. 88, 10754–10758.

Wilkinson, C.D.W., Deng, L., Rahman, M., 2002. Jpn. J. Appl. Phys. 41, 4261–4266.

Zheng, G., Patolsky, F., Cui, Y., Wang, W.U., Lieber, C.M., 2005. Nat. Biotechnol. 23, 1294–1301.

Zhou, X.T., Hu, J.Q., Li, C.P., Ma, D.D.D., Lee, C.S., Lee, S.T., 2003. Chem. Phys. Lett. 369, 220–224.